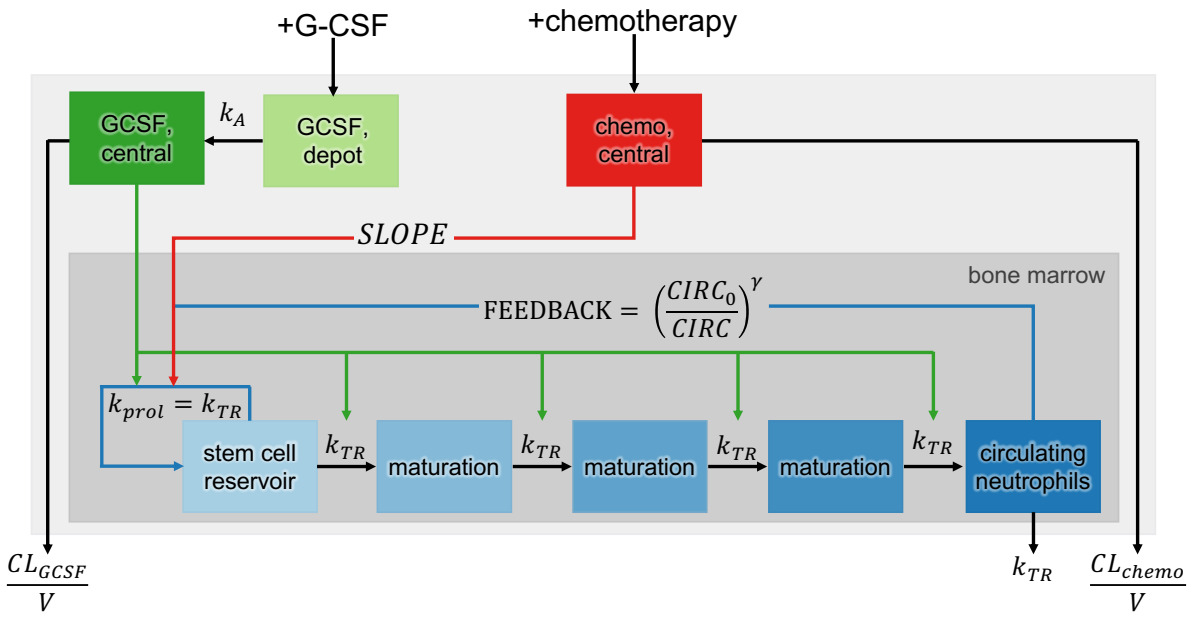

Figure S1: Schematic illustrating the structure of the adapted Friberg model. G-CSF administration was modeled as sub-cutaneous, with an absorption compartment and a central compartment. Chemotherapy was modeled as a bolus dose into a central compartment. Neutrophils were modeled as a stem cell reservoir replenished by proliferation, three transit compartments reflecting the stem cell maturation process, and a circulating neutrophil compartment. The overall mean transit time (MTT) is equal to four divided by the inter-compartment transit rate (k_{TR}). The intercompartmental transit rate is stimulated by GCSF. Proliferation rate is equal to the transit rate multiplied by the drug effect ($SLOPE$ times drug concentration) multiplied by the feedback effect and an additive stimulatory effect of exogenous G-CSF.

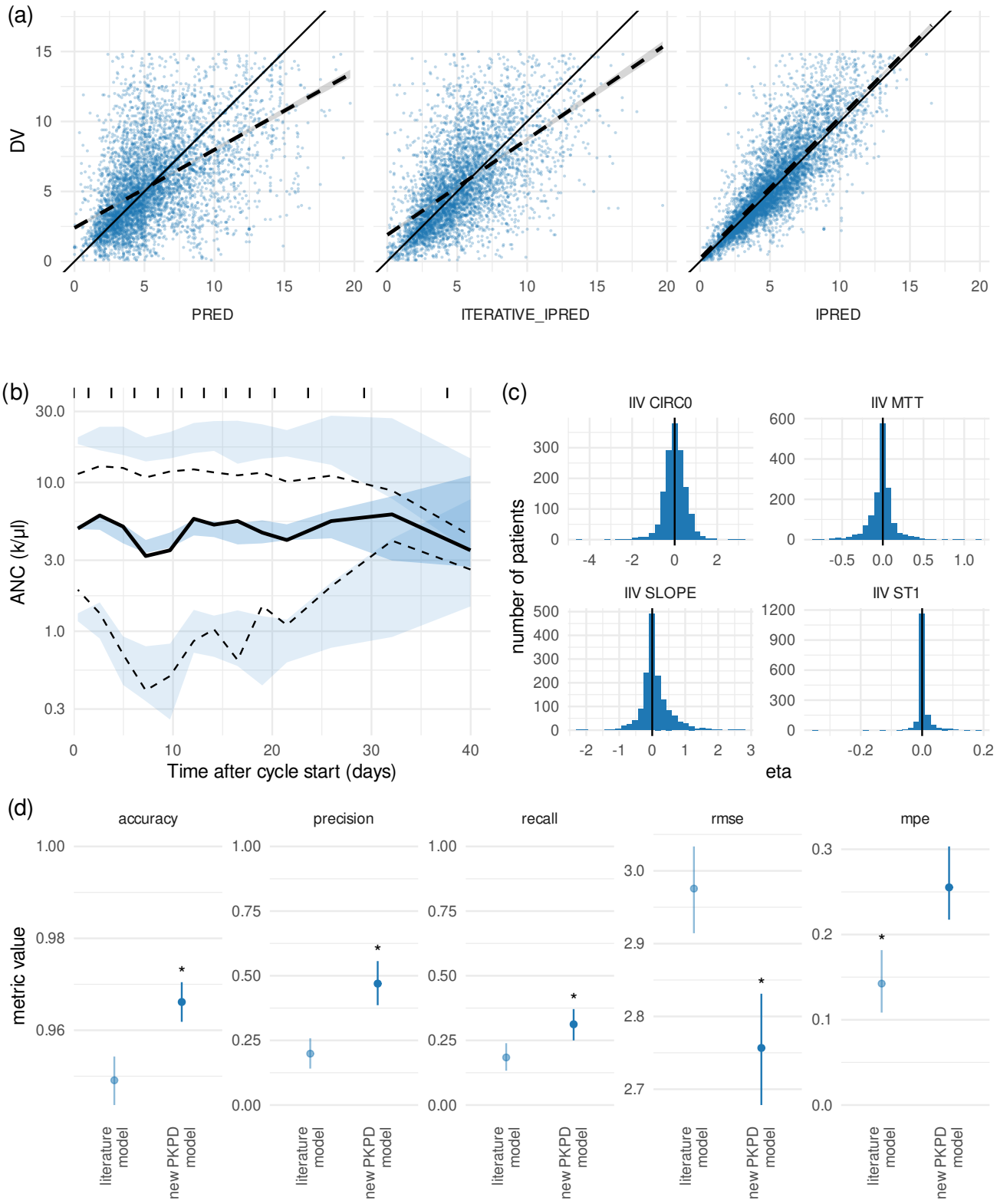

Figure S2: Diagnostic plots for the final PKPD model, evaluated on the test data set. (a) DV-prediction plots for population predictions (PRED), iterative individual predictions computed with PsN proseval (ITERATIVE_IPRED) and individual predictions (IPRED). (b) visual predictive check comparing observed data distributions. Shaded areas indicate the 95% confidence intervals around the 95th, 50th and 5th percentile of simulated data. Black lines indicate the 95th, 50th and 5th percentile of observed data. (c) Distribution of individual eta estimates. (d) Comparison of the new PKPD model with the literature model (Melhem et al, 2018). Prediction performance is summarized according to accuracy, precision, recall, root mean square error (rmse), and mean percent error (mpe). Variability in these error metrics was assessed across 1000 bootstrapped samples; points indicate the median and bars indicate the 5th to 95th percentile of these bootstrapped metrics. Asterisks indicate the model with the best performance on that error metric.

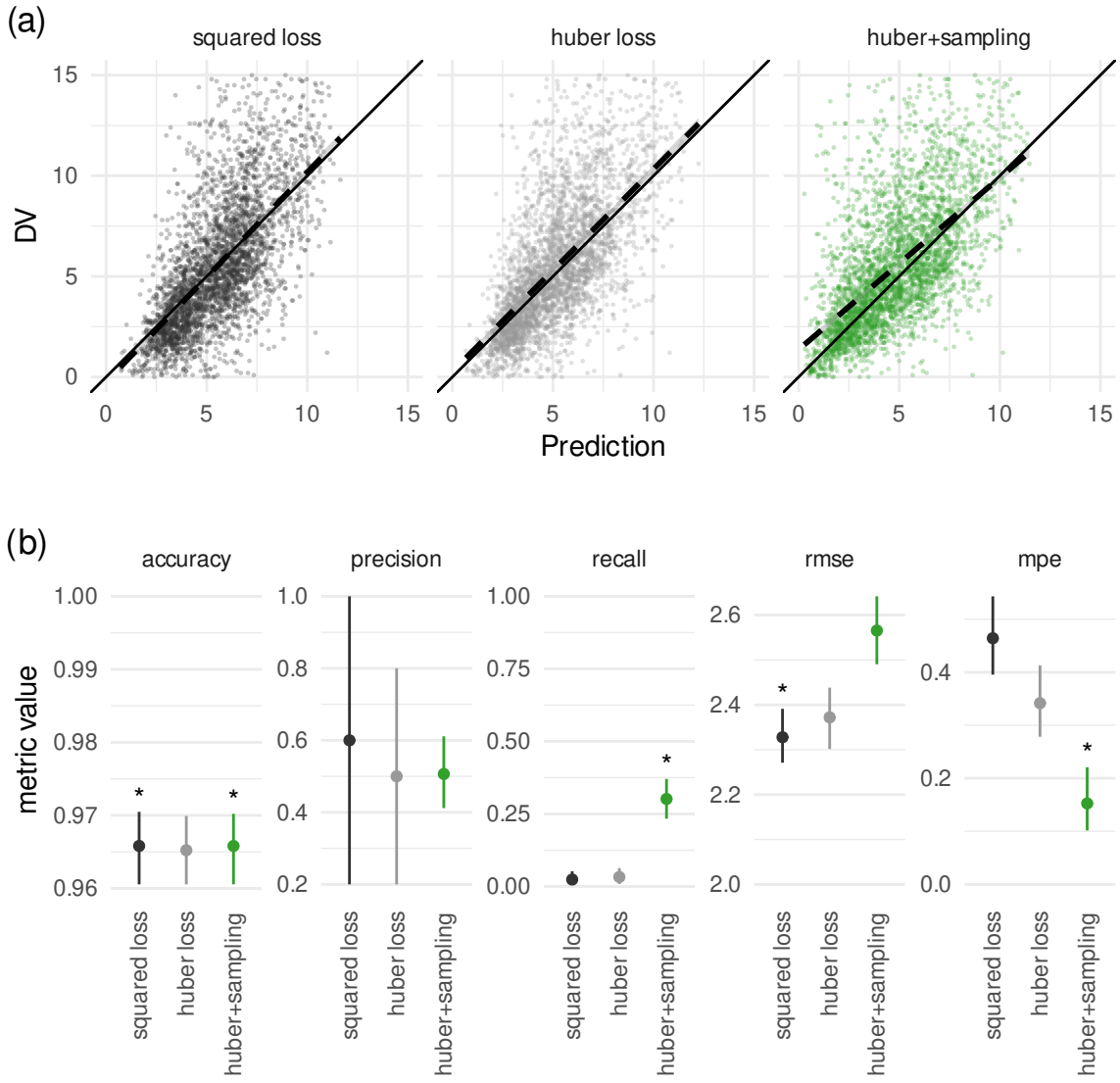

Figure S3: Performance of XGBoost loss functions and subsampling. (a) Comparison of observed (DV) and predicted values for the default (squared error) loss function, the pseudo-Huber loss function and thepseudo-Huber loss function with down-sampling and up-sampling. (b) Performance of the three training conditions on prediction performance as measured by accuracy, precision, recall, root mean square error (rmse), and mean percent error (mpe). Asterisks indicate the training condition with the best performance on that error metric. Variability in these error metrics was assessed across 1000 bootstrapped samples; points indicate the median and bars indicate the 5th to 95th percentile of these bootstrapped metrics.

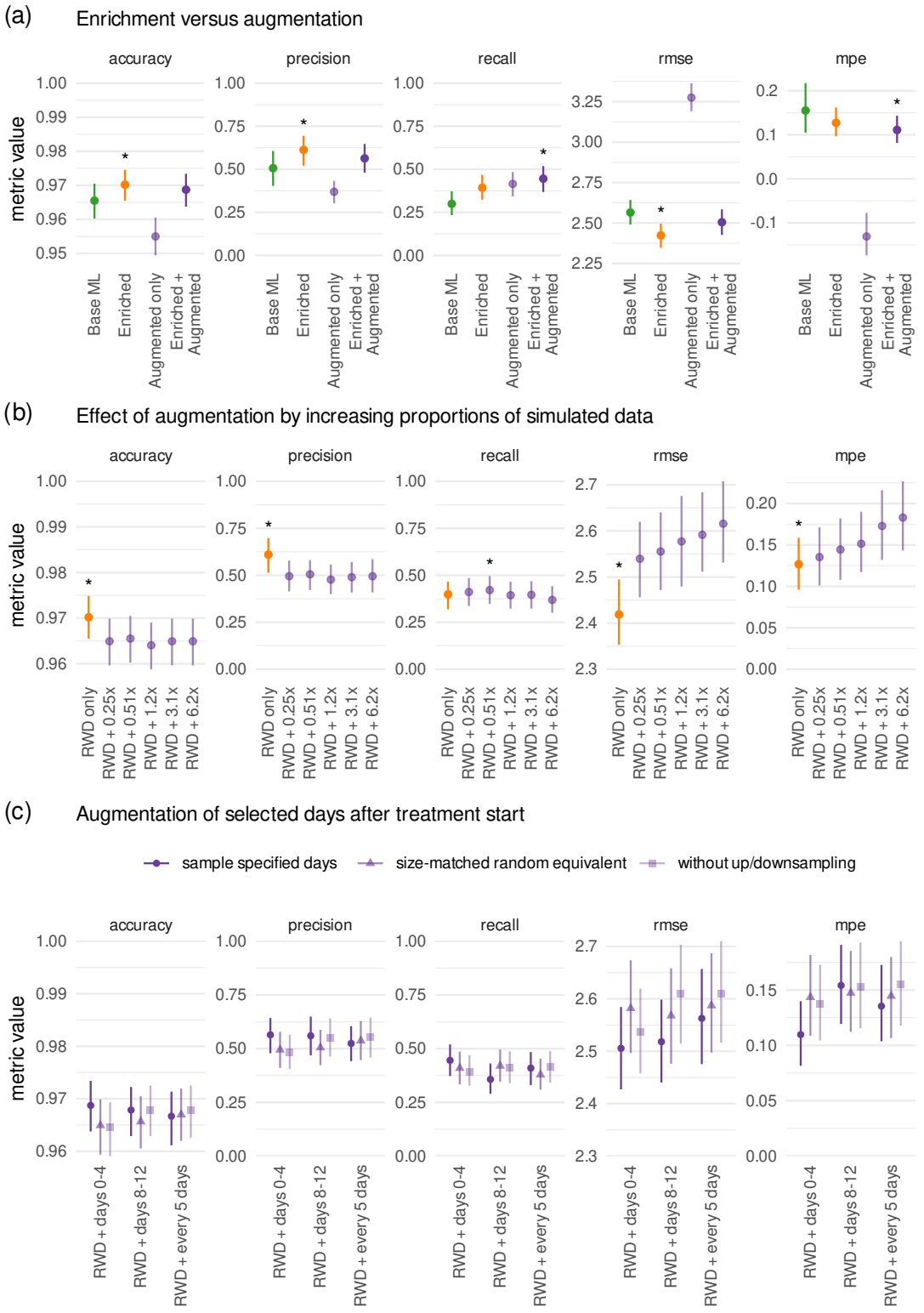

Figure S4: Analysis of factors impacting augmented model performance. (a) Comparison of the base ML model, the enriched model, the base ML model with augmentation (81%) and the enriched model with augmentation (81%). (b) Enriched models with different quantities of augmentation (0%, 25%, 51%, 120%, 310%, 620% additional new simulated data relative to the number of rows of the RWD data set), with simulated data randomly sampled from within the first 3 cycles of chemotherapy. (c) Enriched models with simulated data sampled from different regions of the ANC-time curve (days 0-4, days 8-12, or every fifth day of therapy after each chemotherapy dose). For control, randomly selected rows corresponding to the same fold enrichment (0.81x, 0.52x, 0.91x) are also shown (triangles), as well as size-matched randomized controls without up-sampling and down-sampling (squares). Prediction performance is summarized according to accuracy, precision, recall, root mean square error (rmse), and mean percent error (mpe). For all plots, variability in these error metrics was assessed across 1000 bootstrapped samples; points indicate the median and bars indicate the 5th to 95th percentile of these bootstrapped metrics. Asterisks indicate the training condition with the best performance on that error metric.

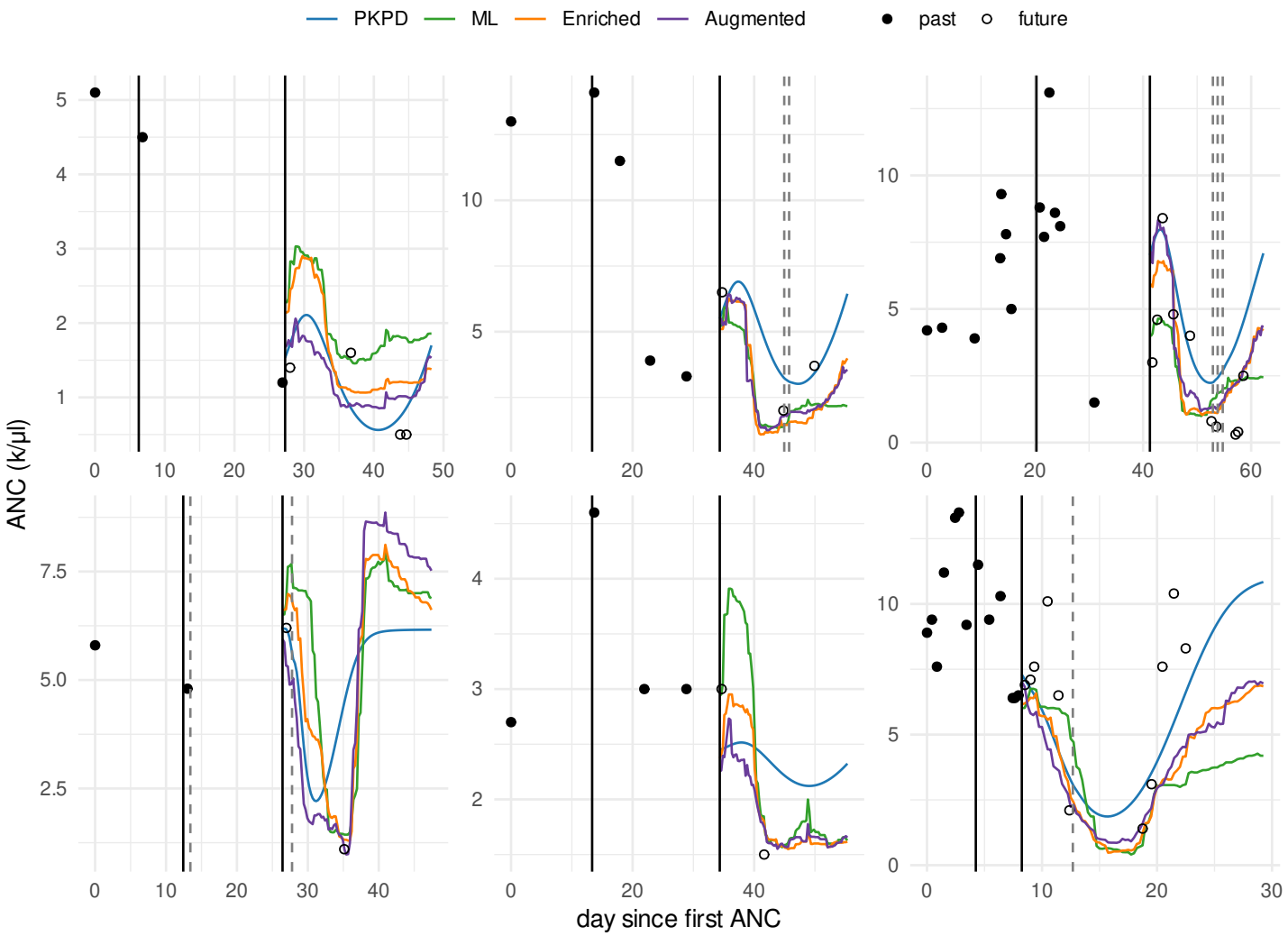

Figure S5: Representative patient treatment courses, with model predictions of ANC over time. At the time of the second cycle, all available data is used to predict future ANCs (open circles). Doses of chemotherapy ar e indicated by solid vertical lines, and administration of GCSF is indicated with dashed grey lines.

Table S1: Literature review for factors predictive of neutropenia

Covariate	References
Height, weight, body surface area	1–6
Sex	1,5,7
Age	1,5–8
Bilirubin	1,7
Serum creatinine, creatinine clearance	4,5
Alpha-1-Acid Glycoprotein	6,7
Ferritin	9
C-reactive protein	9
White blood cell count	10
Alkaline phosphatase	10
Aspartate Aminotransferase	7,10
Serum albumin	7,11
Hemoglobin	12
Oncological surgery	13
HIV status	14

1. Joerger, M. *et al.* Evaluation of a pharmacology-driven dosing algorithm of 3-weekly paclitaxel using therapeutic drug monitoring: a pharmacokinetic-pharmacodynamic simulation study. *Clin Pharmacokinet* **51**, 607–617 (2012).
2. Morita-Ogawa, T., Sugita, H., Minami, H., Yamaguchi, T. & Hanada, K. Population pharmacokinetics and renal toxicity of cisplatin in cancer patients with renal dysfunction. *Cancer Chemother Pharmacol* **86**, 559–566 (2020).
3. Kontny, N. E. *et al.* Population pharmacokinetics of doxorubicin: establishment of a NONMEM model for adults and children older than 3 years. *Cancer Chemother Pharmacol* **71**, 749–763 (2013).
4. Joerger, M. *et al.* Dosing algorithm to target a predefined AUC in patients with primary central nervous system lymphoma receiving high dose methotrexate: High dose methotrexate dosing algorithm. *British Journal of Clinical Pharmacology* **73**, 240–247 (2012).
5. Johansson, Å. M. *et al.* A population pharmacokinetic/pharmacodynamic model of methotrexate and mucositis scores in osteosarcoma. *Ther Drug Monit* **33**, 711–718 (2011).
6. Quartino, A. L., Friberg, L. E. & Karlsson, M. O. A simultaneous analysis of the time-course of leukocytes and neutrophils following docetaxel administration using a semi-mechanistic myelosuppression model. *Invest New Drugs* **30**, 833–845 (2012).
7. Kloft, C., Wallin, J., Henningsson, A., Chatelut, E. & Karlsson, M. O. Population Pharmacokinetic-Pharmacodynamic Model for Neutropenia with Patient Subgroup Identification: Comparison across Anticancer Drugs. *Clinical Cancer Research* **12**, 5481–5490 (2006).
8. Chen, N. *et al.* Pharmacokinetics and pharmacodynamics of *nab* -paclitaxel in patients with solid tumors: Disposition kinetics and pharmacology distinct from solvent-based paclitaxel. *The Journal of Clinical Pharmacology* **54**, 1097–1107 (2014).
9. Razzaghdoust, A., Mofid, B. & Moghadam, M. Development of a simplified multivariable model to predict neutropenic complications in cancer patients undergoing chemotherapy. *Support Care Cancer* **26**, 3691–3699 (2018).
10. Lyman, G. H. *et al.* Predicting individual risk of neutropenic complications in patients receiving cancer chemotherapy. *Cancer* **117**, 1917–1927 (2011).
11. Intragumtornchai, T., Sutheesophon, J., Sutcharitchan, P. & Swasdikul, D. A predictive model for life-threatening neutropenia and febrile neutropenia after the first course of CHOP chemotherapy in patients with aggressive non-Hodgkin's lymphoma. *Leuk Lymphoma* **37**, 351–360 (2000).
12. Morrison, V. A., Caggiano, V., Fridman, M. & Delgado, D. J. A model to predict chemotherapy-related severe or febrile neutropenia in cycle one among breast cancer and lymphoma patients. *JCO* **22**, 8068–8068 (2004).
13. Cao, X. *et al.* Predicting risk of chemotherapy-induced severe neutropenia: A pooled analysis in individual patients data with advanced lung cancer. *Lung Cancer* **141**, 14–20 (2020).
14. Vendrell, I. *et al.* Chemoradiotherapy completion and neutropenia risk in HIV patients with cervical cancer. *Medicine* **97**, e11592 (2018).

Table S2: Description of machine learning model features. Features shaded in grey are presentonly in hybrid models.

Feature	Category	Type	Unit	Description
cycle_anc	ANC	numeric	k/uL	ANC at time of dose
anc_type	ANC	categorical	-	predicted ANC is mid-cycle or on day of next dose
min_anc_ever	ANC	numeric	k/uL	lowest recorded ANC for patient
median_anc	ANC	numeric	k/uL	median of past measured ANCs
var_anc	ANC	numeric	k/uL	variance of past measured ANCs
N_anc_lc	ANC	numeric	-	# ANC measurements in the previous dosing cycle
min_anc_lc	ANC	numeric	k/uL	lowest measured ANC in the previous dosing cycle
race	demographics	categorical	-	race, US Census definitions
ethnicity	demographics	categorical	-	ethnicity, US Census definitions
weight	demographics	numeric	kg	weight of patient
sex	demographics	categorical	-	sex of patient
age	demographics	numeric	years	age in years
cancer	diagnosis	categorical	-	breast, thoracic or lymphoma
doses_to_next	drug	numeric	-	# doses until next measured ANC
gcsf	drug	categorical	-	G-CSF administered this cycle (formulation, or “none”)
num_prev_gcsf	drug	discrete	-	# of previous cycles with G-CSF usage
prop_prev_gcsf	drug	discrete	-	% of previous cycles with G-CSF usage
regimen	drug	discrete	-	chemotherapy regimen for this cycle
n_neutropenic	drug	discrete	-	# neutropenic drugs in chemo regimen
mean_dose	drug	numeric	mg/m^2	dose normalized to body surface area in this cycle
cyclelength	drug	numeric	days	inter-cycle duration
after_cycle3	drug	boolean	-	flag for more than 3 doses into chemo
ALP	labs	numeric	IU/L	alkaline phosphastase lab value at the time of the current cycle
AST	labs	numeric	U/L	aspartate aminotransferase lab value at time of current cycle
bilirubin_total	labs	numeric	mg/dL	total bilirubin at time of current cycle
creat	labs	numeric	mg/dL	serum creatinine lab value at the time of current cycle
serum_albumin	labs	numeric	mg/dL	serum albumin
wbc	labs	numeric	k/uL	white blood cell count
rel_crcl	labs	numeric	$mL/min/1.73m^2$	relative creatinine clearance
surgery	surgery	boolean	-	invasive surgery performed this cycle
d_since_cyclestart	time	numeric	days	# days since last dose of the predicted ANC
d_from_10	time	numeric	days	# days from day 10 post-dose of the predicted ANC
SLOPE	PK/PD	numeric	1/uM	Bayesian individual estimate of SLOPE
MTT	PK/PD	numeric	hours	Bayesian individual estimate of MTT
predicted_anc	PK/PD	numeric	k/uL	Individualized PKPD model prediction
EXPETA4	PK/PD	numeric	-	interindividual variability of G-CSF effect from PKPD model